Scientific Inquiry and Review (SIR)
Volume 7 Issue 1, 2023
ISSN (P): 2521-2427, ISSN (E): 2521-2435
Homepage: https://journals.umt.edu.pk/index.php/SIR

Article QR

Title:	**Image Registration using the Rigid Group**
Author (s):	Muhammad Yousuf Tufail, Saima Gul
Affiliation (s):	NED University of Engineering & Technology, Karachi, Pakistan
DOI:	https://doi.org/10.32350/sir.71.05
History:	Received: November 22, 2022, Revised: February 7, 2023, Accepted: February 7, 2023, Published: March 15, 2023
Citation:	Tufail MY, Gul S. Image registration using the rigid group. *Sci Inq Rev.* 2023;7(1):71–86. https://doi.org/10.32350/sir.71.05
Copyright:	© The Authors
Licensing:	This article is open access and is distributed under the terms of Creative Commons Attribution 4.0 International License
Conflict of Interest:	Author(s) declared no conflict of interest

A publication of
The School of Science
University of Management and Technology, Lahore, Pakistan

Image Registration using the Rigid Group

Muhammad Yousuf Tufail*, and Saima Gul

NED University of Engineering and Technology, Karachi, Pakistan

Abstract

Image registration is the process of approximate matching of the source image to the target so that they resemble each other. In this study, two-dimensional image registration is presented using the rigid group. This group is a finite dimensional group (four-dimensional in this case) under composition. The dimensions of the rigid group are scaling, rotation, and translations along the axes. In this paper, an algorithm for the construction of rigid transformation is presented using the discretized objective function. This objective function is based on SSD (sum of the squares of the distances between the pixels intensities) and calculates the discrepancy between the images. The coarse search and the gradient descent approaches have been used for the optimization. The proposed algorithm is implemented on variety of images. The numerical examples illustrate the ability of the proposed algorithm.

Keywords: algorithms, coarse search, image registration, optimization, rigid group.

1. INTRODUCTION

Image registration is the process of the approximate matching of the source image to the target so that their appearances resemble each other. The pioneer work of D'Arcy Thompson remains the original inspiration in the field of image registration. In his famous book *On Growth and form* [1, 2], which was first published in 1917 and then re-published in 1942, he presented the idea of image transformation between species. Some of the images and their relative transformations that he referred in his book motivated the current authors to further explore finite dimensional group, which is the scope of this paper. Although there have been many developments in image registration since 1942, still the most remarkable and influential approach is to find a diffeomorphism between the two images using a method known as "Large Deformation Diffeomorphic Metric Mapping (LDDMM)" [3–7].

* Corresponding Author: tufail@neduet.edu.pk

Lisa Gottesfeld Brown published the first comprehensive review of image registration in 1992 [8]. Brown highlighted the various requirements of image registration namely (i) a feature space (contains information about the images), (ii) a search space (consists of a set of transformations), (iii) a search strategy (selection of transformations to get an optimal solution), and (iv) a similarity metric (to measure the discrepancy between the images). Brown suggested only three lists of transformations (all were finite) including (a) affine transformation (shearing, aspect ratio, and rigid), (b) perspective transformation (a transformation that maps 3D to 2D), and (c) polynomial transformation (suitable when minor information regarding camera geometry is available [2, 9]). The basic steps in image registration still remain the same. However, the choice of transformations has evolved drastically. The full set of diffeomorphisms, that is, non-rigid registration using infinite dimensional group is an integral part of image registration and widely applied in medical imaging [6–7, 10].

Several methods for image deformation have been developed and applied to the distinct fields of mathematics and computer science since 1992. These methods include artificial intelligence[11], image encryption [12], graph theory, [13] and many more [14–26]. The adoption of diffeomorphic image registration has caused a revolutionary and significant change in the field. Diffeomorphisms refer to those smooth functions whose inverse are also smooth [2, 9, 27].

In this paper, image registration is presented using the group of rigid diffeomorphisms. Two-dimensional grey scale images [2, 9] have been used to conduct the experiments. Image registration is subject to the optimal solution of the current study's objective function which is defined in **Eq. (2.2)**. This equation demonstrates how close the images are. This objective function is based on **SSD** (sum of the squares of the distances between the pixels intensities). For more details, see equation (2.9) in Section 2.2 in [2]).

2. RIGID GROUP AND IMAGE REGISTRATION

The rigid group of diffeomorphisms is one of the most common group which is extensively used in image registration. It has been studied extensively over the past several decades, both for medical and non-medical applications [28–33]. This group consists of uniform scaling, rotations, and arbitrary translations along the axes [8, 19, 34–36]. Let us first present each of these separately.

2.1. Rotation

Suppose an arbitrary point $\begin{pmatrix} X \\ Y \end{pmatrix}$ in $\mathbb{R}^2$. Let $\zeta \in [0,2\pi[$ be the angle of rotation, then the rotation transformation ψ_1 to generate a new point $\begin{pmatrix} X' \\ Y' \end{pmatrix}$ in $\mathbb{R}^2$ is defined as

$$\begin{pmatrix} X' \\ Y' \end{pmatrix} = \psi_1 \begin{pmatrix} X \\ Y \end{pmatrix} = \begin{pmatrix} \cos\zeta & -\sin\zeta \\ \sin\zeta & \cos\zeta \end{pmatrix} \begin{pmatrix} X \\ Y \end{pmatrix}.$$

2.2. Scaling

Suppose $\gamma \in \mathbb{R}^+$, then the scaling transformation ψ_2 over $\begin{pmatrix} X \\ Y \end{pmatrix}$ is represented below as

$$\begin{pmatrix} X' \\ Y' \end{pmatrix} = \psi_2 \begin{pmatrix} X \\ Y \end{pmatrix} = \gamma \begin{pmatrix} X \\ Y \end{pmatrix}.$$

2.3. Translation along the Axes

Suppose $tr_x, tr_y \in \mathbb{R}$ are the translations along the x-axis and y-axis respectively. The translation transformation ψ_3 over $\begin{pmatrix} X \\ Y \end{pmatrix}$ is defined below as

$$\begin{pmatrix} X' \\ Y' \end{pmatrix} = \psi_3 \begin{pmatrix} X \\ Y \end{pmatrix} = \begin{pmatrix} X + tr_x \\ Y + tr_y \end{pmatrix}.$$

The diffeomorphims group generated by the composition of scaling, rotation, and translations along the axes is termed as the rigid group. See **Proposition 2.1** for more details. The composition of individual transformations yields $\begin{pmatrix} X' \\ Y' \end{pmatrix} = \psi\left(\begin{pmatrix} X \\ Y \end{pmatrix}\right)$, where $\psi = \psi_3 \circ \psi_2 \circ \psi_1$

$$\begin{pmatrix} X' \\ Y' \end{pmatrix} = \gamma \begin{pmatrix} \cos\zeta & -\sin\zeta \\ \sin\zeta & \cos\zeta \end{pmatrix} \begin{pmatrix} X \\ Y \end{pmatrix} + \begin{pmatrix} tr_x \\ tr_y \end{pmatrix}, \zeta \in [0,2\pi[, 0 \neq \gamma \in \mathbb{R}^+.$$

The formula to represent the inverse rigid diffeomorphism is defined as

$$\begin{pmatrix} X \\ Y \end{pmatrix} = \frac{1}{\gamma}\begin{pmatrix} \cos\zeta & -\sin\zeta \\ \sin\zeta & \cos\zeta \end{pmatrix}^{-1}\left\{\begin{pmatrix} X' \\ Y' \end{pmatrix} - \begin{pmatrix} tr_x \\ tr_y \end{pmatrix}\right\}, \zeta \in [0,2\pi[, 0 \neq \gamma \in \mathbb{R}^+$$

$$= \frac{1}{\gamma}\begin{pmatrix} \cos\zeta & \sin\zeta \\ -\sin\zeta & \cos\zeta \end{pmatrix}\left\{\begin{pmatrix} X' \\ Y' \end{pmatrix} - \begin{pmatrix} tr_x \\ tr_y \end{pmatrix}\right\}, \zeta \in [0,2\pi[, 0 \neq \gamma \in \mathbb{R}^+.$$

Proposition 2.1. The existence of the composition of rigid diffeomorphisms in the domain $\Omega \subset \mathbb{R}^2$ implies the following fact:

$$(\psi_1 \circ \psi_2) \cdot \big(I(\boldsymbol{x})\big) = \psi_1 \cdot \big(\psi_2 . I(\boldsymbol{x})\big), \forall \psi_1, \psi_2 \in \mathrm{rig}(\Omega, \mathbb{R}^2).$$

Here, '.' denotes the action of ψ over the image I, $\circ$ indicates the composition, see Section 1.2.4 in [2], and the set of rigid diffeomorphisms is represented with rig $(\Omega, \mathbb{R}^2)$.

Proof: Suppose ψ_1 and ψ_2 are rigid diffeomorphisms in Ω such that their composition $\psi_1 \circ \psi_2$ is also a diffeomorphism in Ω, then

$$\begin{aligned}
(\psi_1 \circ \psi_2) \cdot I(\mathbf{x}) &= I((\psi_1 \circ \psi_2)^{-1}(\mathbf{x})) \\
&= I\big((\psi_2^{-1} \circ \psi_1^{-1})(\mathbf{x})\big) \\
&= I(\psi_2^{-1}(\mathbf{x}) \circ \psi_1^{-1}(\mathbf{x})) \\
&= I \circ \psi_2^{-1}(\mathbf{x}) \circ \psi_1^{-1}(\mathbf{x}) \\
&= (I \circ \psi_2^{-1}(\mathbf{x})) \circ \psi_1^{-1}(\mathbf{x}) \\
&= (\psi_2 \cdot I(\mathbf{x})) \circ \psi_1^{-1}(\mathbf{x}) \\
&= \psi_1 \cdot \big(\psi_2 \cdot I(\mathbf{x})\big)
\end{aligned}$$

Definition 2.1. Suppose I_1 and I_2 are two greyscale images. The discrepancy between the images is computed with the following matching functional or objective function

$$M(\psi) = \int_\Omega \{(I_1 \circ \psi^{-1})(\boldsymbol{x}) - I_2(\boldsymbol{x})\}^2 dxdy, \boldsymbol{x} = (X, Y)^T \in \Omega \subset \mathbb{R}^2 \quad (2.1)$$

where ψ represents an element from the rigid group (See Section 2). Then, the process of finding an optimal ψ that minimizes **Eq. (2.1)** is termed as a rigid registration. It is clear that **Eq. (2.1)** is the continuous version of the objective function. As far as numerical computation is concerned, the continuous form is discretized. Suppose we define our discrete domain $\mathbb{D}$. This domain serves as the discrete domain for all the images presented in this paper. Suppose M is a positive integer and $\mathbb{D} = \{([0, M - \alpha]/(M -$

$\alpha) - 0.5) \times ([0, M - \alpha]/(M - \alpha) - 0.5); \alpha = 1\}$ is a uniform square grid that contains M^2 grid points, a simple example by setting $M = 100$ is shown in Figure 1. Consider $M = 100$ for all the numerical examples in this paper. The discrete form of the objective function (defined in **Eq. (2.1)**) is

$$M(\psi) = \sum_{i=1}^{M} \sum_{j=1}^{M} \left((I_1 \circ \psi^{-1})(y_{ij}) - I_2(y_{ij}) \right)^2. \qquad (2.2)$$

Here, y_{ij} indicates the value of the image at position (i, j) in the image matrix.

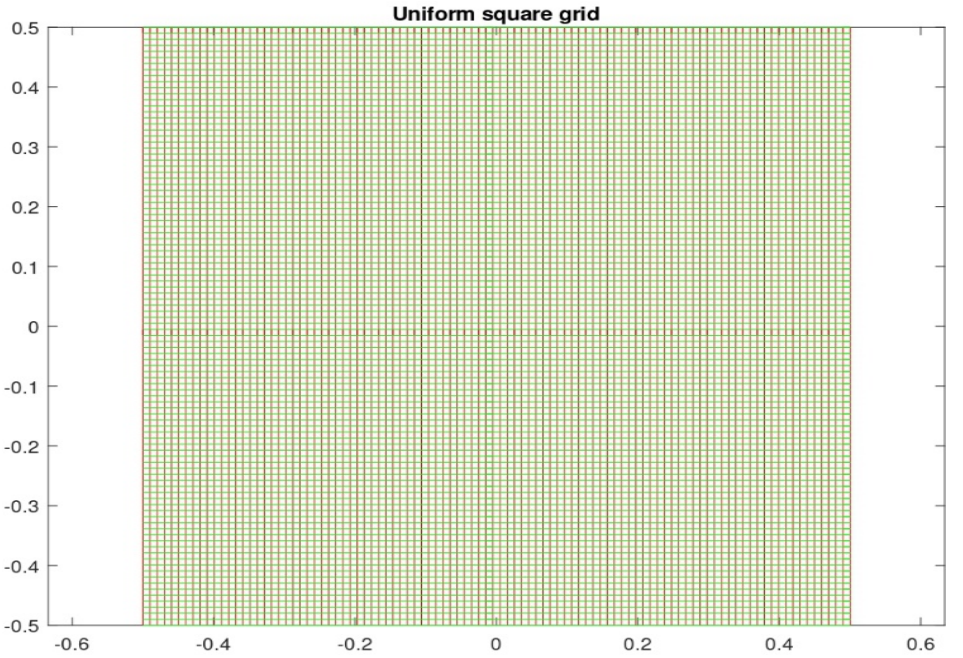

Figure 1. A Total of 10,000 Points for a Square Grid are Given. The range for Data Points is $\left\{[-\beta, \eta] \times [-\beta, \eta]; \beta = \eta = \frac{1}{2}\right\}$, with 100 Grid Points per Side, i.e., $M = 100$.

Moreover, the values of I_1 are defined over the uniform grid points, i.e., at y_{ij} and not at $\psi^{-1}(y_{ij})$. Furthermore, it must be noticed that the domain of $I_1 \circ \psi^{-1}$ is not Ω, instead it is $\psi(\Omega)$ at the continuous level. It is highly likely (for some points) that $I_1 \circ \psi^{-1}$ move outside Ω in the registration. Thus, Ω is a restricted subset of R^2. As far as computation is concerned, the

following values for $I_1 \circ \psi^{-1}(y_{ij})$ are used.

1. If $\psi^{-1}(y_{ij}) \in \Omega$, bilinear interpolation (Section 2.1.2 in [2]) is used by using the values of I_1 corresponding to four neighboring edges of a square that contains $\psi^{-1}(y_{ij})$.
2. If $\psi^{-1}(y_{ij}) \notin \Omega$,, a constant background value (0 for a black background in **Example 4.1** and 1 for a white background in **Examples 4.2** and **4.3**) is set.

The central goal for the registration is to minimize $M(\psi)$ for $\psi \in G$. In this paper, two methods are used for optimization namely (i) the method of coarse search (that surveys the whole discretized domain for all the parameters, four in our case), and (ii) the *trust- region-reflective* method.

The latter method is used when researchers encounter the non-linear least squares problem and it yields a local optimal solution. The trust-region-reflective algorithms have been used through MatLab, see example 4.3 .

Eq. (2.2) denotes the general form of the least-squares optimisation (based on SSD) function for any choice of planar transformation group (i.e., G is a Lie group that acts on the plane [37], G is the rigid group for this study). This is a numerical optimization problem. Optimization is a huge field with many known algorithms [9, 38–40] whose applicability depends on the nature of the objective function. The purpose here is not to survey this field but to demonstrate some simple applications.

3. COARSE SEARCH

In this method, firstly, the domain for the matching functional is defined. This matching functional is computed for several points $\psi \in G$, see **Algorithm 4.1** for further details. This algorithm contains four nested loops, that is, the parameters of the rigid group. The values of individual parameters are set as $M_\zeta = 21, M_\gamma = 13, M_x = 11, \text{and } M_y = 11$. The total search for optimal solution (minimization in this case) is the product of all four nested loops, that is, a total of 33,033 computations for the objective function.

4. EXPERIMENTS

In this section, the implementation of **Algorithm 4.1** over synthetic data is presented. In synthetic data, the target is generated (by using known rigid transformation) from the source. Three examples are presented in which

the first example involves a pair of smooth images, whereas the other two examples are related to the registration of non-smooth images.

Example 4.1 (pair of smooth images). In this first warm-up example, 2D Gaussian blob (an example of smooth image) is considered for image registration. The Gaussian function is considered as the source of image registration. A rigid transformation, with the parameters values $\zeta = \mathrm{pi}/2, \gamma = 0.8, \mathrm{tr}_x = 0.2$ and $\mathrm{tr}_y = 0.4$, are used to generate the target. **Algorithm 4.1** yields the optimized set of parameters whose values are $\zeta_{\mathrm{opt}} = \pi/2, \gamma_{\mathrm{opt}} = 0.8, \mathrm{t}_{x_{\mathrm{opt}}} = 0.2$ and $\mathrm{t}_{y_{\mathrm{opt}}} = 0.4$. These optimised parameters are used to transform the source with a rigid transformation. The transformed source is then subtracted from the target. By doing this, attention is drawn toward the fact that how good the images are aligned (transformed source and the target). Midgrey pixels indicate a perfect match,[1] whereas the evidence of mismatch appears as black (pixel value is ≈ 0) or white (pixel value is ≈ 1). Figure 2 displays the results of registration. An excellent registration is obtained (as expected). The optimal solution is highlighted with a red circle in the bottom part of Figure 2.

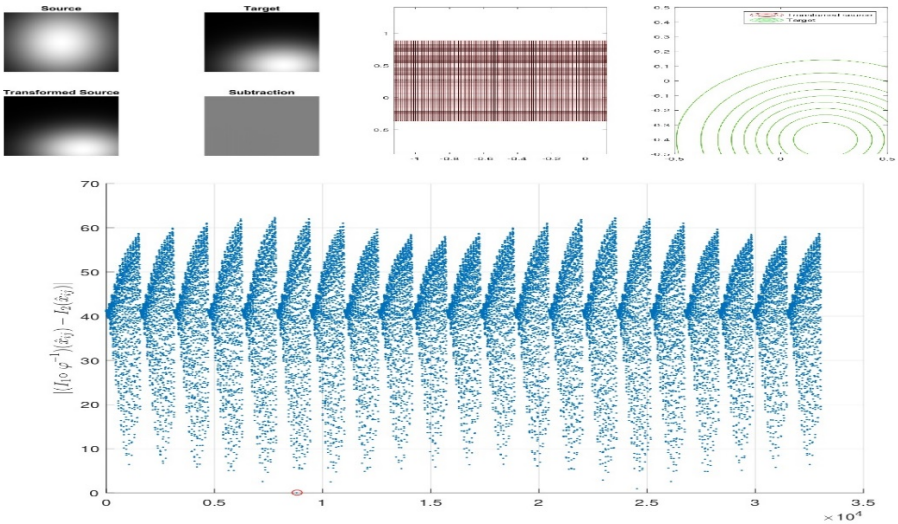

Figure.2. Image Registration is Given for **Example 4.1.** Top: Left: Source

[1] Perfect match here and elsewhere means good visual registration, i.e., there is no mismatch (apparently) between the transformed source and the target; and evidence of midgrey pixels screen when the transformed source is subtracted from its corresponding target.

(the Gaussian $\exp(-5x^2 - 3y^2)$), Target, Deformed Source, and Difference Image $\big((I_1 \circ \psi^{-1} - I_2 + 1)/2\big)$, Uniform Mid Grey Confirms that Perfect Registration between the Images is Obtained; Right: Rigid Diffeomorphism ψ^{-1} Applied to the Target Grid with the Comparison of Contour Plots of $I_1 \circ \psi^{-1}$ (the Transformed Source) and I_2 (the Target). The contour plots Have Been Made by Plotting Green Contours on Top of Red Contours. No Red Line Can Be Seen Due to Perfect Registration. Bottom: The Registration Errors Are Given. The Optimal Solution Is Identified as A Red Circle.

Example 4.2 (**pair of non-smooth images).** Image registration for non-smooth images is always challenging [9]. Consider the pair of non-smooth images. Alike the previous example, again the synthetic data is considered, that is, $\zeta = \mathrm{pi}/2, \gamma = 1.1, \mathrm{tr_x} = -0.2$, and $\mathrm{tr_y} = 0.1$ are set as the initial parameters for the known rigid transformation. The implementation of **Algorithm 4.1** produces optimized parameters that are $\zeta_{\mathrm{opt}} = \frac{\pi}{2}, \gamma_{\mathrm{opt}} = 1.1, \mathrm{t_{x_{opt}}} = -0.2$, and $\mathrm{t_{y_{opt}}} = 0.1$. After obtaining these optimized parameters, the source is transformed by following the same steps as in the **Example 4.1**. The results of image registration are given in Figure 3. Alike the previous example, a perfect registration is obtained.

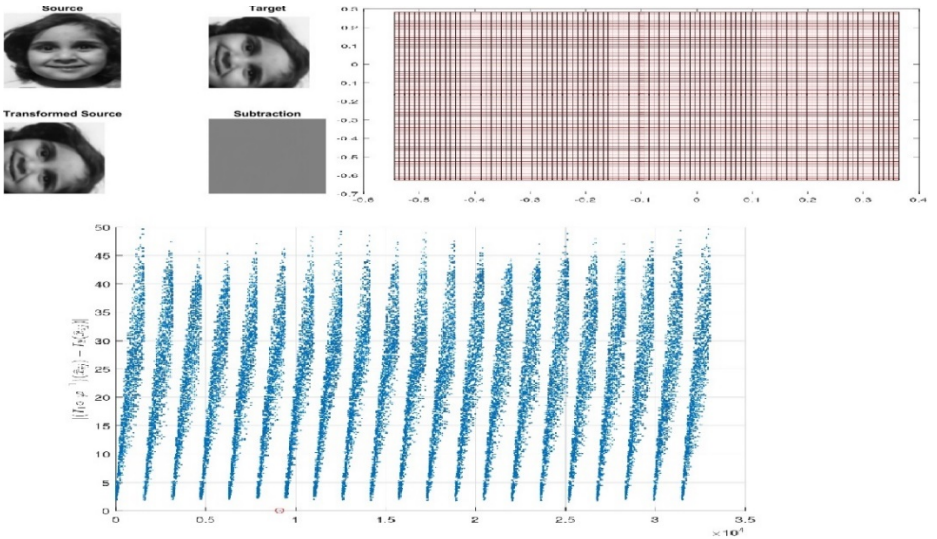

Figure 3. Implementation of **Algorithm 4.1** Over A Pair of Nonsmooth Images Used for **Example 4.2**.

Example 4.3 (pair of non-smooth images). Now consider a slightly harder example in which the target is generated from the source with the help of rigid transformation. The values $\zeta = 1.6, \gamma = 1.25$, $\mathrm{tr}_x = -0.27$ and $\mathrm{tr}_y = 0.13$ are set as parameter values for rigid transformation. Resultantly, **Algorithm 4.1** produced $\zeta_{opt} = \pi/2, \gamma_{opt} = 1.2, \mathrm{t}_{x_{opt}} = -0.3$ and $\mathrm{t}_{y_{opt}} = 0.1$ as optimized parameters. These parameter values are noticeably different from those values of parameters that were used to construct the target. The reason for discrepancy (in values) is due to the fact that the set of allowable values for the parameters in coarse search do not contain the exact values of the parameters that were used to generate the target. Thus, Figure 4 displays adequate but not perfect registration.

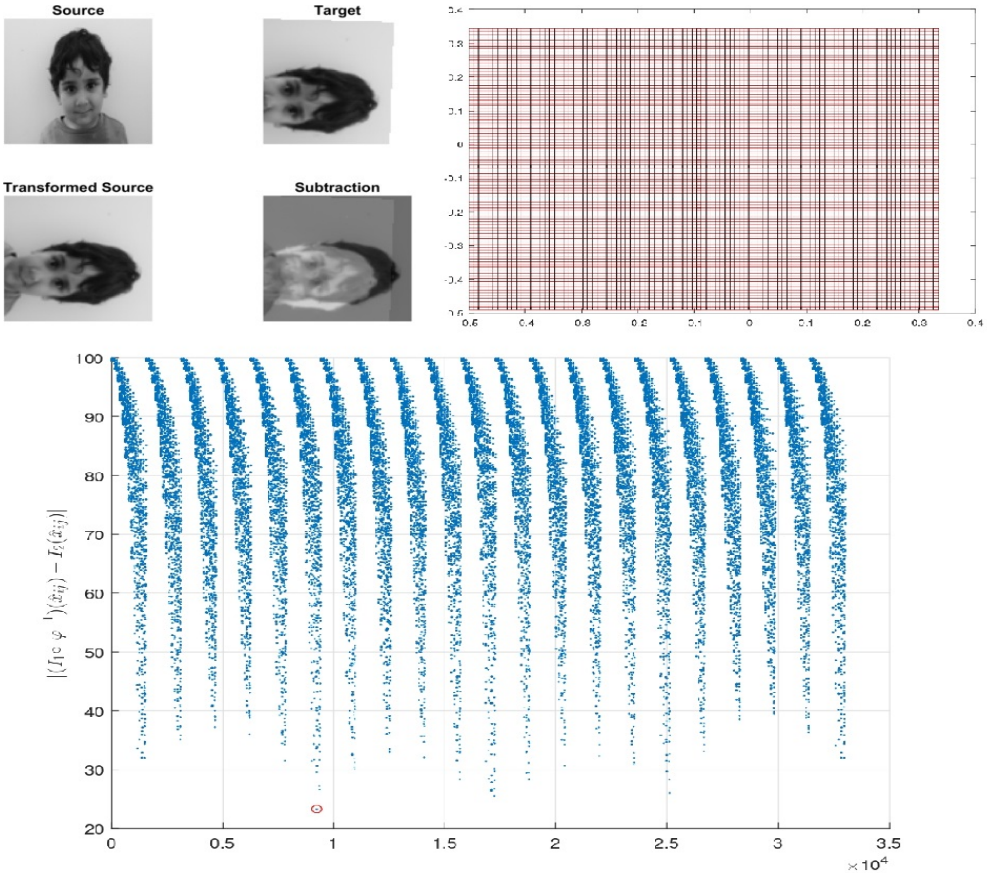

Figure 4. Result of Image Registration Using **Algorithm 4.1** for **Example 4.3**.

MatLab based optimizer **lsqnonlin** is used for the current non-linear problem. This optimizer is used for the (typical) least squares functions for optimization [2, 41].

lsqnonlin requires an initial guess for optimization. For this purpose, the above optimized parameters that were obtained at the first step of optimization (the coarse search), that is, $\zeta_{\text{ini}} = \pi/2, \gamma_{\text{ini}} = 1.2, \mathrm{t}_{\mathrm{x}_{\text{ini}}} = -0.3$, and $\mathrm{t}_{\mathrm{y}_{\text{ini}}} = 0.1$ were chosen as an initial guess. The optimizer yields a global minimum and the corresponding values of the parameters are $\zeta_{\text{opt}} = 1.6, \gamma_{\text{opt}} = 1.25, \mathrm{t}_{\mathrm{x}_{\text{opt}}} = -0.27$, and $\mathrm{t}_{\mathrm{y}_{\text{opt}}} = 0.13$. Figure 5 confirms a perfect registration.

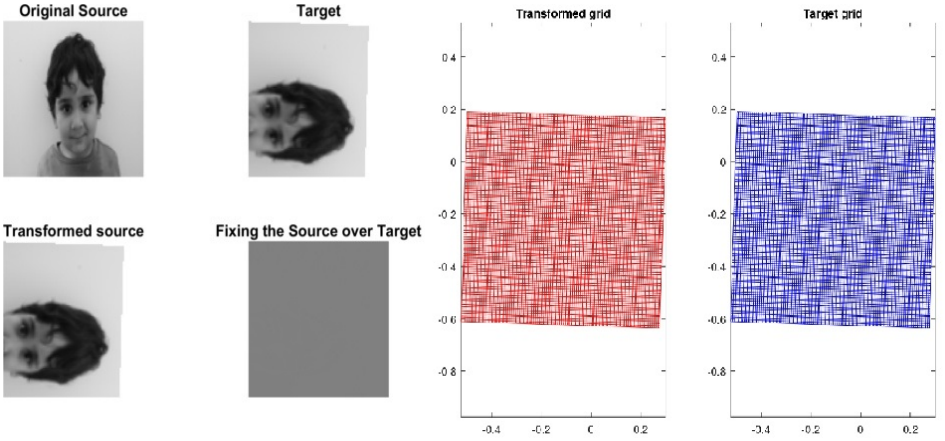

Figure 5. Results of Image Registration for **Example 4. 3** Using Lsqnonlin. Top Row: Pair of Relevant Images for the Registration. Second Row: The Transformed Source ($I_1 \circ \psi^{-1}$) And the Subtraction Between the Transformed Source and The Target. Bottom Row: The Transformed Grid and The Target Grid. These Identical Grids Indicate the Perfect Registration Between the Source and The Target.

Algorithm 4.1. Minimization of **Eq.** (**2.2**) using Coarse Search

Input : Source I_1 and target I_2

output: Warp ψ^{-1} along with the transformed image $I_1 \circ \psi^{-1}$

for $\zeta = 0{:}\,\pi/10{:}\,2\pi$ do

for $\gamma = 0.1{:}\,0.1{:}\,1.3$ do

for $tr_x = -0.5{:}\,0.1{:}\,0.5$ do

for $tr_y == -0.5{:}\,0.1{:}\,0.5$ do

Computation of deformation of source using bi-linear interpolation,

$I_1 \circ \psi^{-1}(x_{ij}) \forall y_{ij} \in S$

Compute $d = \|I_1 \circ \tilde{\psi}^{-1}(x_{ij}) - I_2(x_{ij})\|^2 \forall y_{ij} \in S$

Compute $\psi^{-1} = \tilde{\psi}^{-1}$ for the optimal solution of d,

final deformation of source: $I_1 \circ \psi^{-1}$

5. Conclusion

In this research, an algorithm for the construction of rigid diffeomorphisms has been presented. This algorithm gives an optimal solution for the objective function which calculates the discrepancy between the images (see **Eq. (2.2)**). It worked very well for the selected examples and found the optimal solution for perfect match. However, there is a deficiency in the algorithm that it gets stuck on the local minimum for some examples (not reported here). Due to this deficiency, the current authors were unable to find a perfect match (see Example 4.3). Thus, other optimization techniques are also needed to overcome this deficiency. Gradient descent (there are few more, see [42, 43]) is one of the approaches and used in **Example 4.3**.

The major benefit of the proposed algorithm is that (as it is based on coarse search) it surveys the whole domain and provides a good initial guess for more sophisticated optimization. Apparently, this method is very simple but it is always recommended to search for each parameter (over a relatively small number of values)in the whole domain. In light of modern research on optimization, it is worthy to implement coarse search because (i) it is worthless to compute the derivative at the first step (function might not be differentiable) and (ii) function might have several local minima scattered all over the domain. It becomes nearly impossible for the derivative-based optimization method (such as steepest descent) to find the global minimum. In this situation, the method of coarse search is the best option to get a better initial guess (possibly very near to the global minimum, see **Example 4.3**) in order to find the desired optimal solution for the perfect match.

REFERENCES

[1] Thompson DW. *On growth and form*. Cambridge university press; 1942.

[2] Tufail MY. *Image registration under conformal diffeomorphisms* [doctoral dissertation]. Massey university, Palmerston north, New Zealand; 2017. https://mro.massey.ac.nz/handle/10179/12459

[3] Beg MF, Miller MI, Trouvé A, Younes L. Computing large deformation metric mappings via geodesic flows of diffeomorphisms. *Int J Comput Vis*. 2005;61(2):139–57. https://doi.org/10.1023/b:visi.0000043755.93987.aa

[4] Cao Y, Miller MI, Winslow RL, Younes L. Large deformation diffeomorphic metric mapping of vector fields. *IEEE Transac Med Imag*. 2005;24(9):1216–30. https://doi.org/10.1109/tmi.2005.853923

[5] Glaunès J, Qiu A, Miller MI, Younes L. Large deformation diffeomorphic metric curve mapping. *Int J Comput Vis*. 2008;80(3):317–36. https://doi.org/10.1007/s11263-008-0141-9

[6] Grenander U, Miller MI. Computational anatomy: An emerging discipline. *Quart Appl Math*. 1998;56(4):617–94. https://doi.org/10.1090/qam/1668732

[7] Joshi SC, Miller MI. Landmark matching via large deformation diffeomorphisms. *IEEE Transac Image Proc*. 2000;9(8):1357–1370. https://doi.org/10.1109/83.855431

[8] Brown LG. A survey of image registration techniques. *ACM Comput Surv.* 1992;24(4):325–376. https://doi.org/10.1145/146370.146374

[9] Marsland S, McLachlan RI, Tufail MY. Conformal image registration based on constrained optimization. *NZIAM J*. 2020;62(3):235–55. https://doi.org/10.1017/s144618112000022x

[10] Smith SM, Jenkinson M, Woolrich MW, et al. Advances in functional and structural MR image analysis and implementation as FSL. *Neuroimage*. 2004;23:S208-S219. https://doi.org/10.1016/j.neuroimage.2004.07.051

[11] Ullah W, Siddique I, Zulqarnain RM, Alam MM, Ahmad I, Raza UA. Classification of arrhythmia in heartbeat detection using deep learning.

Comput Intell Neurosci. 2021;2021:e2195922. https://doi.org/10.1155/2021/2195922

[12] Asif M, Mairaj S, Saeed Z, Ashraf MU, Jambi K, Zulqarnain RM. A novel image encryption technique based on mobius transformation. *Comput Intell Neurosci*. 2021;2021:e1912859. https://doi.org/10.1155/2021/1912859

[13] Dayan F, Javaid M, Zulqarnain M, Ali MT, Ahmad B. Computing banhatti Indices of hexagonal, honeycomb and derived networks. *American J Math Comput Model*. 2018;3(2):38–45. https://doi.org/10.11648/j.ajmcm.20180302.11

[14] Grzeszczuk R. An Approach to classifying data with highly localized unmarked features using neural networks. *Comput Sci*. 2019;20:329–42. https://doi.org/10.7494/csci.2019.20.3.3343

[15] Gupta A. Current research opportunities for image processing and computer vision. *Computer Science*. 2019;20(4):387–410. https://doi.org/10.7494/csci.2019.20.4.3163

[16] Dabbour AA, Habib R, Saii M. Object pose estimation in monocular image using modified FDCM. *Comput Sci*. 2020;21(1):97–112. https://doi.org/10.7494/csci.2020.21.1.3426

[17] Chen K. *Introduction to variational image-processing models and applications*, 2013;90(1):1–8. https://doi.org/10.1080/00207160.2012.757073

[18] Frasczek R, Cyganek B, Wiatr K. Parallelized algorithms for finding similar images and object recognition. *Comput Sci*. 2013;14(1):113–127. https://doi.org/10.7494/csci.2013.14.1.113

[19] Zitova B, Flusser J. Image registration methods: a survey. *Image Vis Comput*. 2003;21(11):977–1000. https://doi.org/10.1016/s0262-8856(03)00137-9

[20] Glasbey CA, Mardia KV. A review of image-warping methods. *J Appl Statis*. 1998;25(2):155–171. https://doi.org/10.1080/02664769823151

[21] Kryjak T, Komorkiewicz M, Gorgon M. Real-time moving object detection for video surveillance system in FPGA. Paper presented at: *Conference on Design & Architectures for Signal & Image Processing*; November 2–4, 2011; Tampere, Finland.

https://doi.org/10.1109/dasip.2011.6136881

[22] Bartoli G. Image registration techniques: A comprehensive survey. *Visual Information Processing and Protection Group*; 2007. https://citeseerx.ist.psu.edu/document?repid=rep1&type=pdf&doi=b6d9d5785a425a86097956c508908228106863ac

[23] Goshtasby AA. *Image registration: Principles, tools and methods*. Springer; 2012.

[24] Ogiela MR. Methods of the Straightening Transformation and Analysis of Outer Contours of Objects in Medical Image Recognitio. *Comput Sci*. 1999;1(1):103–112. https://doi.org/10.7494/csci.1999.1.1.3574

[25] Ogiela MR. Fitting of tonal curve and balancing of gray levels in contrast expansion and preliminary imaging of structures in the analysis. *Comput Sci*. 2000;2:81–92. https://doi.org/10.7494/csci.2000.2.0.3580

[26] Saxena S, Singh RK. A survey of recent and classical image registration methods. *Int J Sig Proc Image Process Pattern Recog*. 2014;7(4):167–76. https://doi.org/10.14257/ijsip.2014.7.4.16

[27] Younes L. *Shapes and diffeomorphisms*. Berlin: Springer; 2010. https://doi.org/10.1007/978-3-642-12055-8

[28] Hill DL, Batchelor PG, Holden M, Hawkes DJ. *Medical image registration. Phy Med Biol*. 2001;46(3):R1. https://doi.org/10.1088/0031-9155/46/3/201

[29] Kotsas P, Dodd T. Rigid registration of medical images using 1D and 2D binary projections. *J Dig Imag*. 2011;24(5):913–925. https://doi.org/10.1007/s10278-010-9352-z

[30] Goshtasby AA. *2-D and 3-D image registration: for medical, remote sensing, and industrial applications*. John Wiley & Sons; 2005.

[31] Knaan D, Joskowicz L. Effective intensity-based 2D/3D rigid registration between fluoroscopic X-ray and CT. *Med Image Computi Comput-Assis Interven.* 2003;351–358.

[32] Livyatan H, Yaniv Z, Joskowicz L. Gradient-based 2-D/3-D rigid registration of fluoroscopic X-ray to CT. *IEEE Transactions on medical imaging*. 2003;22(11):1395–406.

https://doi.org/10.1109/tmi.2003.819288

[33] Yaniv Z. Rigid registration. *Image-Guid Interven*. 2008:159–92. https://doi.org/10.1007/978-0-387-73858-1_6

[34] Jenkinson M, Smith S. A global optimisation method for robust affine registration of brain images. *Med Image Anal*. 2001;5(2):143–56. https://doi.org/10.1016/s1361-8415(01)00036-6

[35] Modersitzki J. *FAIR: Flexible algorithms for image registration*. Society for Industrial and Applied Mathematics; 2009.

[36] Denton ER, Sonoda LI, Rueckert D, et al. Comparison and evaluation of rigid, affine, and nonrigid registration of breast MR images. *J Comput Assist Tomo*. 1999;23(5):800–805. https://doi.org/10.1097/00004728-199909000-00031

[37] Abdel-All NH, Abdel-Razek MA, Abdel-Aziz HS, Khalil AA. Geometry of evolving plane curves problem via lie group analysis. *Stud Math Sci*. 2011;2(1):51–62.

[38] Chong EK, Zak SH. *An introduction to optimization*. John Wiley & Sons; 2013.

[39] Mirjalili S, Lewis A. The whale optimization algorithm. *Adv Eng Soft*. 2016;95:51–67. https://doi.org/10.1016/j.advengsoft.2016.01.008

[40] Kirmani SK, Jamil RN. Optimization of complex geometry using tenth order partial differential equation. *Sci Inq Rev*. 2018;2(2):23–31. https://doi.org/10.32350/sir/22/020203

[41] Inc. The MathWorks. Optimization Math Toolbox: https://au.mathworks.com/help/optim/ug/lsqnonlin.html?searchHighlight=lsqnonlin&stid=srchtitle . Natick, Massachusetts, United State, 2020.

[42] Rashid M, Iqbal MA, Noor NA. DFT-mBJ study of electronic and magnetic properties of cubic CeCrO3 compound: an ab-initio investigation. *Sci Inq Rev*. 2017;1(1):27–36. https://doi.org/10.32350/sir/11/010104

[43] Iqbal MA, Erum N. Opto-Electronic investigation of rubidium based Fluoro-Perovskite for Low Birefringent Lens Materials. *Sci Inq Rev*. 2017;1(1):37–48. https://doi.org/10.32350/sir/11/010105